Energy, Mines and Resources Canada

Énergie, Mines et Ressources Canada

CANMET

Canada Centre for Mineral and Energy Technology

Centre canadien de la technologie des minéraux et de l'énergie

Metals Technology Laboratories

Laboratoires de la technologie des métaux

Canada

METALS TECHNOLOGY LABORATORIES

91-03592/

NUMERICAL ANALYSIS OF A FLAWED PRESSURE VESSEL

A.S. ODDY AND J.M.J. MCDILL

MTL 90-45(TR)

MICROMEDIA

30 pp

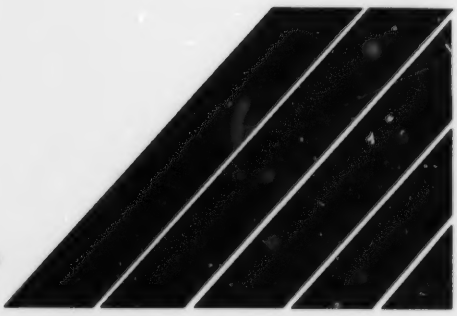

METALS TECHNOLOGY LABORATORY
REPORT MTL 90-45(TR)

NUMERICAL ANALYSIS OF A FLAWED PRESSURE VESSEL

by

A.S. Oddy and J.M.J. McDill

ABSTRACT

The analysis of four defects in the pressure vessel selected for the Engineering Critical Assessment of a flawed vessel is presented. Nonlinear, elastoplastic, finite deformation, finite element analysis of the defects thought to be most likely to cause failure was accomplished as the first stage in the assessment. Three independent determinations of the severity of the conditions at the crack tip and therefore the risk of fracture were made. These were based on the J integral, using a virtual crack advance technique, the crack tip opening displacement (CTOD), from the displacements calculated around the crack tip, and a continuum damage analysis. Plastic collapse predictions were also made. For the defects analysed it was found that there was no danger of fracture at pressures less than that required to cause general plasticity. Indeed a very simple check showed that the uncracked ligaments were all too small to properly contain the plasticity around the crack tip. Thus ductile failure is the only possible failure mechanism and single parameter characterizations such as J or CTOD are not valid. Plastic collapse was predicted to occur at a pressure greater than 11 MPa.

LABORATOIRE DE LA TECHNOLOGIE DES MÉTAUX
RAPPORT MTL 90-45(TR)

ANALYSE NUMÉRIQUE D'UN RÉCIPIENT À PRESSION DÉFECTUEUX

par

A.S. Oddy et J.M.J. McDill

RÉSUMÉ

Le rapport fait état de l'analyse de quatre défauts présents dans le récipient sous pression choisi à des fins d'évaluation technique critique d'un récipient défectueux. La première étape de l'évaluation comportait une analyse de déformation finie, élastoplastique et non linéaire ainsi qu'une analyse élémentaire finie des défauts susceptibles de causer la rupture. On a fait trois déterminations indépendantes de la gravité des conditions à l'extrémité de la fissure et, par conséquent, du risque de fracture. Ces déterminations sont fondées sur l'intégral J, déterminé à l'aide d'une technique de propagation apparente, de la fissure, sur l'ouverture critique de fissuration, déterminée en calculant les déplacements autour de l'extrémité de la fissure, et sur une analyse du dommage en continu. On a aussi fait des prévisions en matière d'écroulement plastique. Pour ce qui est des défauts analysés, on a déterminé qu'il n'existe aucun danger de fracturation à des pressions inférieures à la pression requise pour provoquer la plasticité générale. En effet, une vérification très simple a montré que les ligaments intacts étaient trop petits pour bien contenir la plasticité autour de l'extrémité de la fracture. Cette rupture ductile constitue le seul mécanisme de rupture possible et les caractérisations à un seul paramètre, comme l'intégral J ou l'ouverture critique de fissuration, ne sont pas valables. On peut s'attendre à ce qu'il y ait rupture plastique à une pression de plus de 11 MPa.

INTRODUCTION

The critical assessment of the risk of failure in a pressure vessel was the primary reason for the formation of the Industry/CANMET group on Pressure Vessels, ECA Validation program. As part of this program, the analysis of a flawed pressure vessel was to be performed by several investigators and the predicted failure pressures compared with the results of a full-scale pressurized burst test. Non-destructive examinations of the vessel established the location and size of the defects. An initial assessment of the flaw severities was performed by Jutla et al. [1]. Further numerical analysis was to be undertaken. This report contains the results of one such investigation.

A typical vessel, removed from service, was selected so that any analysis would deal with real flaws, and real vessel geometries. These tend to be more realistic and much more complicated than the long axial flaws artificially induced in other investigations. The primary goal of the analysis was to predict the pressure at which failure occurs, failure being defined as either plastic collapse or the onset of crack propagation.

The vessel selected was formerly a debutanizer donated by Syncrude. The vessel itself was 5.8 m high, 1.8 m in diameter with a wall thickness of 25 mm. A schematic diagram of the vessel is shown in Fig. 1. The vessel was made of ASME SA 516 Grade 70 steel. Some reworking of the vessel, e.g. welding caps on access ports and nozzles, had to be done to prepare it for the burst test.[2]. The additions were designed for a nominal burst pressure of 12.8 MPa.

The use of numerical techniques by several different investigators provides several secondary benefits. The most obvious is to check the accuracy of handbook solutions for idealized conditions when applied to more complex situations encountered in reality. Are these simple calculations and the assumptions needed to justify their application sufficiently accurate to be used as an initial screen? Are they too conservative, or not conservative enough? Is the ranking of their severity accurate?

Another benefit of having several different investigations of the same flaws is to determine if typical engineering practice can produce a consensus on the risk associated with typical flaws. If predictions vary greatly then further guidance will be required before such critical assessments can become routine.

The technique outlined by Garwood et al. [3], where various analytical or empirical expressions are used, is one valid method to determine failure pressures. Rather than follow this technique, it was decided that nonlinear, incremental, finite deformation, elastoplastic finite element analyses of several of the flaws would be worthwhile. Numerical analyses of this sort have the advantage of being able to include several effects not easily included in closed form solutions. Stress concentrations as a result of local geometric effects are one such. Another related effect is the presence of bending stresses created by section changes, flanges or rings etc., additional radial

restraints or even the flaws themselves. Plasticity, and the effects of having more than one material present, i.e., weld deposits vs base plate, can also be included. The effects of bulging and pressure on the crack face may also be included. Finally, plastic collapse of the vessel will be influenced by the formation of plastic hinges, localized regions where plasticity is enhanced because of local conditions. This is also difficult to predict using closed form solutions.

Three independent criteria were used to predict the onset of crack growth. The first was the energy release rate determined by the virtual crack extension based on the J integral [4]. The second was the crack-tip opening displacement (CTOD). The third was based on the continuum damage mechanics relation of Lemaitre [5]. The onset of plastic collapse will be automatically predicted by the elastoplastic analysis. As a general rule, the conditions analysed were intended to be conservative. That is, the conditions were more severe than in reality, and the material properties were selected to promote failure. A full three-dimensional (3D) analysis had originally been intended. However, because of the number of flaws examined, it was not possible to examine them all without reducing them to 2D situations. Some of the flaws examined could be represented as 2D situations with little error. For others, axisymmetric or plane strain analyses represent situations somewhat more severe than actually experienced. The geometry of the various flaws is taken from the initial assessment of Jutla et al. [1].

As will be seen, the fracture properties measured experimentally were significantly larger than those assumed initially. The validity of the initial analyses and their assumptions can be checked by comparing them with the numerical results, using the lower values for fracture properties. This will provide an important check on the accuracy of those initial predictions and help determine what confidence can be granted to typical engineering practice.

A final point to be established is the nature of the prediction being made. The work demonstrated here is not intended to be a prediction of the failure pressure for the vessel in service. When in service, the material is probably saturated with hydrogen. This will reduce the fracture properties considerably. Material properties were taken from room temperature tests of unsaturated material. It will also be evident that no safety factor is applied in any of the predictions. This work is not intended to make any prediction of the safe operating pressure. The sole purpose of the work described here is the prediction of the failure pressure during the burst test. Failure is taken as the onset of crack propagation in any of the defects or the plastic collapse of the vessel.

FAILURE CRITERIA

As mentioned earlier, two broad types of failure are considered. Failure is assumed to occur if any of the cracks start to grow or if plastic collapse occurs. Crack growth might be due to slow stable growth or more rapid catastrophic failure. No attempt was made to distinguish between slow stable crack growth and rapid, unstable crack growth. Prediction of the failure as

the onset of slow stable crack growth is certainly conservative. Prediction of instabilities is difficult because critical quantities, which grow extremely rapidly near instability, are frequently influenced by minor imperfections, or differences in geometry and mechanical properties that are often below the threshold of measurement.

Plastic collapse of the vessel can occur in several forms. They all share a common characteristic in that small increases in pressure cause very large increases in the strains and displacements. General collapse of the unflawed vessel, unlimited plasticity at any of the various flaws or the development of plastic hinges as a result of local bending are all possible. In mathematical terms, collapse occurs when the work done by the applied forces and incremental displacements exceeds the ability of the structure to absorb or dissipate energy through elastic and plastic deformation. In elastoplastic finite element analyses, the approach of plastic collapse is manifested as the rapid growth of displacements and the failure to achieve convergence. If the unrestrained plasticity occurs near the crack being investigated, quantities influenced by the strains and displacements will also grow rapidly.

For the analyses described here, the onset of general plastic deformation in the unflawed vessel was taken to be the largest pressure the vessel was ever likely to experience. For thin-walled vessels, the wall deforms plastically when

$$P = \frac{2}{\sqrt{3}} \sigma_y \ln\left(\frac{R_o}{R_i}\right) \qquad \text{Eq 1}$$

According to Faupel [6], general collapse or bursting of an unflawed vessel can be estimated by

$$P = \frac{2}{\sqrt{3}} \sigma_y \left(2 - \frac{\sigma_y}{\sigma_{uts}}\right) \ln\left(\frac{R_o}{R_i}\right) \qquad \text{Eq 2}$$

where σ_y is the yield strength, σ_{uts} is the tensile strength, R_i and R_o are the inner and outer radii respectively and P is the pressure. Equation 2 has not been derived using plasticity theory to predict the collapse. It stems from the observation that collapse occurs at a pressure between the value predicted by Eq 1 and the value predicted when σuts is used in Eq 1 in place of σ_y. The ratio of σ_y/σ_{uts} is used as the weighting factor to interpolate between the two limits. Faupel [6] states that this formula is accurate to plus or minus 15%, on a 95% certainty basis.

The rate at which the material work hardens is also important if a rigorous prediction of the collapse pressure is to include the effect of strain hardening. For this reason, Eq 2 is only an estimate since two materials with similar strengths may harden at very different rates.

Three independent criteria were calculated and used in the fracture prediction. The first was the energy release rate based on the virtual crack extension. The second was the calculation of the crack tip opening displacement (CTOD). The third was based on the continuum damage integral of Lemaitre [5].

It is well known that the energy release rate is an alternative definition of the J integral. This definition of the *J* integral assumes a deformation theory of plasticity which really implies nonlinear but elastic behaviour. Thus J increases as the strains increase and becomes very large if plastic collapse is occurring near the crack tip. The calculation of this quantity using the virtual crack advance technique was implemented in the ASGARD finite element code using the relation proposed by Lamain [4]. Numerical predictions of J were to have been used in conjunction with a J-R curve to predict the initial crack growth. As will be seen, this was not possible. Because the calculation of J is an energy-based concept, mesh coarseness is less of a problem than with other criteria.

The elasto-plastic analysis of a cracked structure will directly produce an estimate of the CTOD since displacements are calculated for every node on the crack face. The CTOD is measured at the point of tangency where the crack face curves as a result of the crack tip blunting. This requires a very fine mesh in order to capture the displacements near the crack tip accurately. This makes it the least accurate of the three methods used. Experience in the past has shown that using the method outlined by Karami et al. [7] to determine the linear elastic stress intensity using the crack face displacements requires elements as small as 1/16 of the crack length. This rule-of-thumb was adopted for use in creating the finite element meshes.

The fracture mechanism for ductile materials is one of void initiation, growth and coalescence in the material at the crack tip. Thus the plastic deformation near the crack tip causes the accumulation of damage to the material until a critical value is exceeded, when voids link up and the crack extends.

Lemaitre [5] has proposed a scalar continuum damage variable D, for isotropic damage based on the effective surfacic density of micro-defects on a representative volume element or, in other words, the area of cracks and cavities per unit area. Thus D = 0 corresponds to the completely undamaged state and D = 1 corresponds to the complete separation of the volume into two parts. Using the thermodynamic potential and the thermodynamics of irreversible processes, the rate of evolution of the damage D is

$$\dot{D} = \frac{D_C}{(\varepsilon_R - \varepsilon_D)} \left[\frac{2}{3}(1+\nu) + 3(1-2\nu)\left(\frac{\sigma_n}{\sigma_{eq}}\right)^2 \right] \varepsilon_P^{2n} \dot{\varepsilon}_P \qquad \text{Eq 3}$$

Five material properties appear in Eq 3. Two of them, ν, or Poisson's ratio and the strain hardening coefficient, n, are familiar. The others, D_C, ε_R, ε_D relate to the material's capacity to sustain damage. D_C is the critical value of D at which the voids and microcracks link up, ε_R is the plastic strain at rupture for a uniaxial tensile test and ε_D is the plastic strain required to initiate voids in a uniaxial tensile test. The plastic strain is ε_P and $\dot{\varepsilon}_P$ is the plastic strain rate. The triaxiality ratio of the hydrostatic stress, σ_h, to the equivalent stress, σ_{eq}, also appears.

It can be seen that damage occurs only as a result of plastic deformation. In addition, the damage variable of Lemaitre specifies that damage is negligible until a certain amount of plastic deformation, ε_D, occurs. Thereafter D grows until it reaches the critical value D_C whereupon the voids link up and failure occurs. If D is normalised by D_C and Eq 3 is rearranged it is possible to create a measure of the ductility D' such that

$$D' \int \left[\frac{2}{3}(1+\nu) + 3(1-2\nu)\left(\frac{\sigma_h}{\sigma_{eq}}\right)^2 \right] \varepsilon_P^{2n} \, d\varepsilon_P \qquad \text{Eq 4}$$

Rupture of the material will occur when

$$D' = (\varepsilon_R - \varepsilon_D) \qquad \text{Eq 5}$$

The number of material properties needed to describe rupture in the material has been reduced to two, ε_R and ε_D. If we propose $(\varepsilon_R - \varepsilon_D)$ as a measure of the ductility of the material it is obvious that this can be obtained from a uniaxial tensile test

$$\varepsilon_R - \varepsilon_D = \frac{1}{(2n+1)} \varepsilon_R^{2n+1} \qquad \text{Eq 6}$$

It is a simple matter to incorporate the continuum damage relation shown in Eq 4 into a finite element program in order to predict the failure of elements at the crack tip. As in the other fracture criteria, the damage will increase rapidly if plastic collapse occurs near the crack.

Analysis of crack problems requires that the mesh be sufficiently fine to capture the singularity at the crack tip but not so fine that the assumption of a continuum is invalid. As Mudry [8] states, at the crack tip the plastic strain is infinite, and therefore rupture is inevitable no matter how low the applied load is. Since the presence of voids and microcracks ahead of the crack tip is related to the size and distribution of inclusions, any damage function must be computed at some characteristic distance from the crack tip in order to preserve the assumption that a continuum exists. For a similar damage model Mudry [8] recommends the use of elements of no smaller than approximately 0.2 mm size at the crack tip.

MATERIAL PROPERTIES

As in any assessment, the establishment of the relevant material properties is an essential part of the analysis. The initial investigation by Jutla et al. [1] was forced to estimate the mechanical properties of the vessel. They selected values of 340 MPa and 380 MPa as representative values for the yield strength of the cylindrical shell and domed end caps respectively. A critical CTOD value of 0.031 mm was taken for the fracture properties throughout. This is equivalent to a plane strain energy release rate of J equal to 19.2 N/mm. These fracture properties are quite conservative.

Measurements of the elastoplastic properties for weld metal and base plate material were obtained from several samples cut from the vessel. Naturally some variability in the mechanical properties was observed. The material properties used in the analyses were chosen as those which maximized the severity of the conditions.

The applied conditions corresponded to a load-controlled situation. That is, pressure, the independant variable, is imposed on the vessel and the displacements and strains are the dependent variables. In such a case as this, for a given pressure, materials with lower yield strengths will result in greater plasticity. Since the J integral is based on a deformation theory of plasticity, the lower the yield strength is, the greater the value of J will be for the same force loading. Of course the situation is reversed for displacement controlled loading. Maximizing the applied J is achieved by using the material with the lower yield strength for the conditions to be examined. Similarly, material with a lower yield strength will experience a larger CTOD. Finally, the continuum damage factor of Lemaitre [5] is based on the integral of the plastic strain and it too will be enlarged by using a lower yield strength. Similar arguments can be made for the effect of changes in the hardening modulus.

Rather than pick and choose from amongst the various properties, the elastoplastic material properties were selected from the sample showing the lowest yield strength. The values used are shown in Table 1. Because true stress/true strain curves were not available, the hardening modulus was estimated by using the ultimate tensile strength and the strain hardening exponent to

obtain approximate values for the true stress and true strain at necking. The hardening moduli shown are rather low. Estimation of the hardening modulus in this way underestimates the amount of work hardening which occurs in the early stages of plastic deformation.

Table 1. Elastoplastic material properties. ASME SA 516 Gr 70 steel.

Material	Yield strength (MPa)	Tensile strength (MPa)	Hardening modulus (GPa)	Strain hardening exponent	Ductility D'
Plate	305.8	579.4	0.37	0.4186	0.54
Weld	404.3	589.8	1.26	0.3247	0.63

The preceeding discussion on the effect of lowering the yield strength should not be taken to imply that materials with lower yield strengths are more prone to crack propagation. Lowering the yield strength, for a constant applied force only, increases the applied J or CTOD. The amount of crack propagation experienced for a given J or CTOD is a further material property unrelated to this discussion.

Using the properties in Table 1 and the relations expressed in Eq 1 and 2 it can be seen that the unflawed, cylindrical vessel wall will plastically deform when the pressure reaches approximately 11 MPa. In addition, general plastic collapse is predicted at 16 MPa. Naturally the plastic collapse pressure is only an estimate, minor imperfections will no doubt cause local, nonuniform yielding to occur with some reduction in strength. Finally, plastic collapse pressures will be underestimated if the work hardening is too low.

Fracture properties in the form of experimental J-R curves were also obtained. Crack blunting was assumed to follow

$$J = 2\,\sigma_{\eta}\,\Delta a \qquad \text{Eq 7}$$

J_1, the value at which slow stable crack growth starts was calculated, and the results are shown in Table 2. The equivalent crack-tip opening displacement is also shown in Table 2, calculated from

$$CTOD = \frac{J}{[2\,\sigma_y(1-\nu^2)]} \qquad \text{Eq 8}$$

The flow stress of the weld metal was used for the HAZ samples as well since it was larger than the value for the plate. Larger values of the yield strength reduce both the amount of blunting and the value obtained for J_1.

Table 2. Fracture properties. ASME SA516 Gr 70 steel.

Specimen	Orientation of sample with respect to circumference	Material (N/mm)	J_1 (mm)	CTOD
W-1	transverse	weld	62	0.084
W-2	transverse	weld	188	0.26
W-4	transverse	HAZ	165	0.22
W-6	transverse	HAZ	210	0.29
W-14	parallel	plate	255	0.46
W-15	parallel	plate	120	0.22
W-16	parallel	plate	177	0.32
W-18	transverse	plate	261	0.47
W-19	transverse	plate	271	0.49

The relevant fracture properties for axial flaws are those taken from samples oriented parallel to the circumferential welds. The properties to apply to circumferential defects are those taken in the transverse direction. The minimum value obtained in each group will be used in the fracture prediction. The smallest values for the plate material are for samples taken parallel to the circumference where J_1 is 120 N/mm and the equivalent CTOD is 0.22 mm. For the weld metal the lowest values are from the transverse samples at J_1 equal to 62 N/mm (CTOD 0.084 mm).

The values for J_1 and CTOD shown in Table 2 are all considerably greater than was originally assumed [1]. This means that the likelihood of fracture is much less than originally anticipated. The danger of plastic collapse is enhanced. In fact, a very simple test exists which shows that elastoplastic fracture is not possible for any of the defects, that ductile failure is the only failure mechanism possible. Unfortunately this test was not applied until after the analyses were all complete.

The use of single parameter measures like J or CTOD to characterise the conditions at the crack tip depends on the existence of the Hutchinson-Rice-Rosengren (HRR) singularity around the crack tip. The existence of this singularity requires that the plastic strains be limited to a small region around the crack tip. Specifically, the plastic zone size must be a small fraction of the uncracked ligament. When the ligament is too small, plasticity is not contained to the crack tip, and

shear bands form at approximately 45° to the plane of the crack. In such a case, the HRR singularity does not dominate, and single parameter measures such as J and CTOD are invalid. The stress and strain fields become strongly dependent on the geometry and loading. In practical terms, the energy required to cause crack growth increases.

It is a fairly simple matter to check that the ligament is large enough to create the necessary restraint. Although this should have been the starting point in any analysis, it was unfortunately overlooked and not applied until after the analysis was complete. The uncracked ligament can be non-dimensionalized as

$$M = \frac{c\,\sigma_y}{J_1} \qquad \text{Eq 9}$$

where c is the uncracked ligament, σ_y is the yield stress and J_1 is the material's toughness. The minimum value of M which allows the HRR singularity to develop depends on the loading. This value varies from as low as 50 when the ligament is loaded in bending, up to 200 or more for cases where the ligament is subjected primarily to tension [9]. Since the loading is primarily tensile, it is trivial to show that none of the defects pass this test. Therefore it is quite simple to see that ductile failure is the only possible failure mode. J and CTOD are no longer valid measures of the conditions around the crack tip. Lemaitre's continuum damage factor is still applicable since it can be evaluated at every point in the structure and is therefore not a single parameter measure of the severity of the fields enclosing the crack tip.

DEFECTS ANALYSED

Figure 1 is a schematic diagram of the vessel used and shows the general location of the defects examined. Four of the eleven flaws examined in [1] were selected for further numerical analysis. In effect that report was used as a preliminary screen to assess the severity of the flaws present. The selection was based on three criteria. The first criteria was the risk determined in that examination. The second was the possibility of local bending stresses. The additional radial restraint of section changes, rings or flanges welded to the vessel will create local bending stresses. The third criteria was the presence of stress concentrations near the flaws. Based on these criteria, the demister ring, the circumferential splitter plate flaw, weld C1 axial flaw, and manway flaw 1 were selected.

The axial flaw at weld C3 was not included because discussions revealed that it was not, in fact, a planar flaw but rather 'C' shaped in plan. There was some suspicion that this was

the result of an earlier repair of a hydrogen blister. The flaw shape assumed in [1] was therefore felt to be very conservative.

The initial prediction of the pressure necesary to cause failure at manway flaw 4 was felt by Jutla et al. [1] to be overly conservative. These defects were not examined since failure of the vessel from the propagation of these cracks was not thought likely [1].

Manway flaw 2 is parallel with, and quite close to, manway flaw 1. Since parallel cracks tend to reduce the severity of each others conditions, it was felt that the analysis of only one defect would be conservative.

Nonlinear incremental finite deformation elastoplastic finite element analysis of the demister ring flaws, circumferential splitter plate flaws, weld C1 axial flaw and manway flaw 1 were performed. Although a 3D analysis was possible for any one flaw, the fact that no single flaw was overwhelmingly worse than any other meant that the examination of 4 flaws was necessary. This is not a serious handicap since realistic situations of this sort invariably involve more than one flaw. The 2D analyses could be used to decide which flaws are worthy of a 3D elastoplastic analysis.

In keeping with the recommended mesh requirements outlined above, the size of the smallest elements around the crack tip are approximately 1/16 of the crack length and on the order of 0.2 mm. The 4 to 8 node grading quadrilaterals of McDill [10] were used to intensively grade the meshes around the crack tips. The refined meshes were generated using the automatic mesh refinement algorithm of McDill [11]. Selective reduced integration was imposed in order to avoid locking during plastic deformation and thus permit the prediction of plastic collapse pressures.

CIRCUMFERENTIAL DEMISTER RING FLAW

Fully circumferential flaws exist on either side of the demister ring welded inside the vessel. The presence of this ring provides additional radial stiffness. When the vessel is pressurized, the local radial displacement will be less than in adjacent portions of the vessel wall. This will induce bending stresses in the vessel wall. This bending will create an additional contribution to axial stresses present. Depending on the location, bending will enhance or reduce the axial tensile stresses present. Axial tensile stresses on the inner surface will be increased near the demister ring and reduced further away.

Cracks exist on both sides of the demister ring almost completely around the circumference. It is therefore possible to model this flaw as an axisymmetric case and assume that a plane of symmetry exists down the middle of the demister ring. The dimensions of the fillet welds and crack depth were obtained from [1]. Consideration of a sufficient portion of the vessel wall is necessary to ensure the development of the local bending stresses. Figure 2 shows the mesh used. The lower boundary is the plane of symmetry. The crack faces and the inner surface of

the vessel are subjected to the pressure while a traction equal in magnitude to the axial stress is applied to the upper end. Figure 3 shows a close-up view of the mesh near the crack tip.

Figure 4 shows J, the energy release rate, calculated for the demister ring flaws. Figure 5 shows the CTOD calculated. For a circumferential defect such as this, the relevant fracture properties should be taken from the transverse plate samples listed earlier. Figure 6 shows how the radial displacement of the vessel wall, at some distance from the demister ring, increases with pressure.

The results of the analysis were quite interesting. Convergence occurred quite rapidly for all steps where the pressure was less than 11.5 MPa. All steps above this pressure failed to converge and radial displacements increased rapidly. Element failure from ductile damage at the crack tip occurred when the pressure rose above 12.5 MPa. The rapid rise in J, CTOD and the radial displacements for pressures above about 12 MPa is also evident. These results are clearly indicating that plastic collapse through the development of a plastic hinge at the demister ring and by general collapse of the vessel wall is the likely failure mechanisms at this defect.

The maximum pressure expected in the burst test is 12.8 MPa. Therefore fracture at this defect is not expected. A plastic hinge may develop at the demister rings when the pressure exceeds 11.5 MPa. The work hardening of the material used in the analysis is insufficient to allow much pressurization over the value needed to cause yielding of the vessel wall.

An interesting side light is the difference that bending has made when compared to the results of Jutla et al. [1]. Even with fracture properties as low as those used in the initial analysis (J_1 = 19.2 N/mm, CTOD = 0.031 mm), fracture is unlikely. With these properties crack growth would not start until 11 MPa. This is just before plastic collapse occurs and somewhat greater than the value 8.0 MPa initially predicted. The bending stresses are evidently making a contribution to the severity of the conditions at the crack tip. In this case it is a favourable contribution.

CIRCUMFERENTIAL SPLITTER PLATE FLAW

The splitter plate and its circumferential defect are quite long, approximately 0.965 m long in the circumferential direction. Propagation of the crack through the thickness of the vessel is also much more likely and more serious than any extension of the crack in the circumferential direction. In view of this consideration, an axisymmetric analysis of this defect was considered acceptable.

Figure 7 shows the mesh used for this defect. The right-most surface is the external surface of the vessel. The lower end of the vessel wall was fixed in the vertical direction. Figure 7 shows a close-up view of the mesh around the crack tip.

Pressure loading was applied to all internal surfaces, including the crack faces. A surface traction equal to the axial stress was applied to the upper end of the vessel wall. The

pressure was increased incrementally to a maximum of 10.5 MPa. Increasing the pressure beyond this value was not worthwhile since plastic collapse at the demister ring is predicted for pressures greater than 11 MPa.

The energy release rate, J, for this defect is shown in Fig. 9 and the predicted CTOD shown in Fig. 10. Both figures clearly show that there is no danger of fracture at this defect. As in the demister ring, even if the fracture properties were as low as was assumed in the initial analysis there would still be no fracture at this defect

WELD C1 AXIAL FLAW

The axial flaw in weld C1 is a partial penetration flaw approximately 38.2 mm long and 5.08 mm deep. This crack should really be analysed in 3D but time did not permit it. It was instead, treated as a 2D plane strain situation. The mesh used is shown in Fig. 11. Pressure was applied to the crack face and to the inner surface of the vessel. Tangential displacements at the plane of symmetry were not permitted. Treatment of this flaw in this way involves several approximations. First, the crack is being idealized as a very long crack, much longer than in reality. Thus the restraint provided by uncracked material on both sides in the axial direction will not be present. This represents a serious overestimation of the severity of the situation, particularly with respect to bending at this defect. The results of Saarenheimo et al. [12] show that 2D analyses of even very long cracks (Aspect ratio > 20) significantly overestimate the radial deflection at the crack and thus overestimate the bending that occurs.

A plane strain analysis of this sort will create tensile axial stresses but they will be lower than the actual stresses present. This will reduce the strain energy somewhat, and will lower the value of J predicted. This is not anticipated to be a major effect.

It was not until after the analysis was complete that it was discovered that this flaw was actually at the place where end caps are joined to the cylindrical vessel. The domed endcaps appear to have a short cylindrical collar around the edge. Thus the welded joint itself is not at the junction between the cylindrical and domed endcaps. Local bending at this junction creates a complex pattern of bending stresses. Bending contributions to the axial and hoop stresses alternate from tension to compression depending on the location (inside or outside) and proximity to the joint. The presence of this crack however argues in favour of it being in a region of elevated tensile hoop stresses.

Figures 12 and 13 show the energy release rate and applied CTOD calculated for the axial flaw at weld C1. Both quantities increase to the point where failure by crack propagation might be a possibility. Since the maximum depth of this flaw appears to be in the base plate rather than the weld metal or HAZ the fracture properties used were those taken from sample W-15 in Table 2. Thus J_1 was 120 N/mm and the CTOD for the onset of crack growth was 0.22 mm.

Using these quantities, Fig. 12 suggests that crack propagation will occur at a pressure of slightly over 7.25 MPa. Figure 13 suggests that the critical CTOD is not reached until over 9 MPa. The continuum damage factor of Lemaitre indicates rupture of material at the crack tip occurs at slightly under 7.5 MPa. The agreement between fracture based on the energy release rate and on continuum damage is quite good. The prediction of failure using the CTOD is higher probably because the mesh is too coarse at the crack tip, thus underestimating the displacements that occur during the severe plastic deformation.

As Fig. 14 demonstrates, the plane strain analysis of this partial penetration crack caused a great deal of bending to occur in the ligament, even at very low pressures. The conditions analysed are probably much more severe than those seen in reality. The finite length of this axial flaw will not permit the degree of bending seen in the analysis.

Figure 15 shows the plastic strain field at the crack tip at 7.5 MPa. The plastic zone has become a significant fraction of the ligament. The use of a single parameter such as J or CTOD as a criterion for the onset of crack propagation rests on the assumption that the crack tip field can be described by a one parameter singular field known as a Hutchinson, Rice and Rosengren (HRR) field. An HRR field can be said to exist when the plastic zone is small compared to the ligament. Shih et al. [9] have shown that for cases where the crack is subjected to bending the HRR field exists only when the ligament exceeds 25 to 50 times J/σ_y). For other loading cases an even larger value is recommended. For the conditions examined here the ligament is only 60 times J/σ_y when the pressure is 7.5 MPa. Therefore this defect is in the transition region between elastoplastic fracture and ductile failure.

If the fracture properties had been as low as initially assumed by Jutla et al. [1] then crack growth would be predicted at just over 3.5 MPa (based on J) or slightly under 3.5 MPa (based on CTOD). This is quite a bit lower than the 7.8 MPa predicted by Jutla et al. [1]. On one hand the numerical analysis overestimates the bending occurring at the crack, whereas the initial assessment ignores it. The correct situation will lie in between. However this does illustrate a potential hazard.

MANWAY FLAW

By far the most complicated geometry is associated with the cracks surrounding the manway. The intersection of the pipe and vessel wall, the reinforcement added around the manway and the various welds made either during fabrication or apparently in previous repairs not only make for a complex geometry but make any sort of simple analysis very difficult. The number and size of the defects associated with the manway make it a natural focus for suspicion.

There are some aspects of the geometry which lend some comfort. The initial prediction of the fracture pressure for manway flaw 4 does seem very conservative. The suspicion

that catastrophic failure from these defects is unlikely [1] seems quite reasonable. For these reasons no further examination of these defects was considered. The very large defects, manway flaws 1 and 2 run roughly parallel to one another and therefore will tend to reduce the severity of the conditions at their mid-lengths. The fact that the additional reinforcement added to the outside creates a layered structure which would prevent complete penetration if manway flaw 1 were to grow also works against catastrophic failure. Finally, as part of the preparation for the burst test, a cap was welded over the outside end of the manway. The offset in the internal forces produced by the manway cap should produce bending stresses in the vessel wall that tend to close cracks on the inner surface of the vessel wall. This, and the location of the cracks at welds leads to the suspicion that the cracks are present mainly because of the residual stresses created during welding. If we accept that previous hydrotests have effectively removed any residual stresses [1], then it follows that there is very little to cause further crack growth. In any case, it was decided that the analysis of manway flaw 1 should be attempted.

Two dimensional analyses of the manway flaw 1 will entail considerable abstraction of the actual geometry in order to permit any analysis at all. The types of analysis possible break down to two cases. The first is a plane strain analysis of a section through the centre of the manway, perpendicular to the crack. In such an analysis, pressure would be applied to the inside of the manway and a traction would be applied to the far boundary of the vessel wall. In this case, the bending stresses would definitely tend to close any cracks on the inner surface. Little is to be gained from an analysis of this type.

The alternative is to do an axisymmetric analysis, axisymmetric with respect to the axis of the manway. Analyses of this type have been attempted before when trying to determine the stress concentration factor due to nozzles in heavy-walled pressure vessels [13]. That investigation recommended that the inner diameter of the vessel be increased to 3.2 times its true value and in effect analyse a spherical vessel. It is possible to produce a good estimate of the maximum stress in the nozzle by doing this. This will be a very conservative case for the conditions found here. First, manway defect 1 is sensitive to the axial stress, not the hoop stress. Second, enlarging the diameter overestimates the hoop stress by a factor of 3.2. Thus the nominal stress at the crack is probably 6.4 times the actual value. Finally, any crack in an axisymmetric analysis is, in fact, assumed to do a complete circuit of the vessel. This extremely conservative situation was examined. This too will probably involve bending stresses which will tend to close cracks on the inner surface but the axisymmetric nature of the geometry makes this less certain.

Figures 16 and 17 show the geometry used in the axisymmetric analysis. Pressure loading was applied all over the inner surface of the vessel, manway and the surface of the crack. Radial displacements were not permitted where the top and bottom touch the plane of symmetry.

Figures 18 and 19 show the energy release rate and applied CTOD calculated for these conditions. It is evident from these figures that there is virtually no chance of crack propagation

from this defect. Plastic deformation becomes noticeable at approximately 2.0 MPa, and plastic collapse becomes a problem at 6.0 MPa. The fact that both J and CTOD remain low during plastic collapse is an indication that a plastic hinge is being formed elsewhere, at some distance from the crack. The occurence of plastic collapse in this analysis at 6.0 MPa is of no significance to the burst test of the real vessel. The low value is probably due to the exaggerated radius, 3.2 times the actual value, used in the analysis.

CONCLUSIONS

1. The use of a single value criteria such as J or CTOD to predict fracture in the chosen vessel is invalid. The uncracked ligament is too small to properly contain the plasticity to the crack tip. In such a case, the size and shape of the plastic zone is strongly dependent on the geometry and loading. The assumption that an HRR singularity exists at the crack tip is not valid and single value fracture criteria such as J and CTOD are not meaningful. Ductile failure at these defects through the formation of shear bands is still possible. The prediction of ductile failure requires the calculation of some continuous measure throughout the body since the precise location and size of the shear bands is not known beforehand.
2. The use of Lemaitre's continuum damage factor shows promise in the prediction of ductile failure where single parameter characterizations such as J and CTOD are not valid.
3. Failure at most of the flaws examined is very unlikely. Only the axial flaw in weld C1 showed any possibility of crack growth. Given the rather conservative conditions assumed for that defect it can be said with some confidence that crack propagation will not occur at all below 7 MPa. Even then the plastic zone is a substantial fraction of the uncracked ligament, indicating that ductile failure is more likely. The degree of conservatism inherent in that analysis makes crack propagation unlikely.
4. Analytical expressions of the pressure needed to initiate plasticity and cause plastic collapse predict that plastic deformation will occur at 11 MPa with general collapse at 16 MPa. The numerical results suggest that plastic collapse will occur fairly soon after the onset of plasticity at a pressure of 11 MPa. A more accurate prediction of the elastoplastic response of the vessel would have been possible had a true stress-true strain description of the material been available. Without such information, the prediction of the amount of over pressurization possible before plastic collapse occurs is uncertain.
5. The initial estimates of the fracture pressure made by Jutla et al. [1] appear, in general, to be quite conservative. The only exception to this was the axial flaw at weld C1 where it was assumed that there was no bending component to the load applied at the crack. The numerical analysis presented here shows that substantial bending. The conditions analysed do tend to

exaggerate the amount of bending. Nevertheless, bending at this defect may be significant and should probably not be ignored.

ACKNOWLEDGEMENTS

The authors would like to express their gratitude to Dr. J.A. Goldak of Carleton University, Ottawa, Ontario, for allowing the use of the software and computing facilities and to acknowledge the assistance of A. Chakravarti and T. Jutla of the Materials Technology Centre, Fleet Technology, Kanata, Ontario. The work of R. Bouchard and C. Trinque in measuring the material properties is also gratefully acknowledged.

REFERENCES

1. Jutla , T. and Chakravarti, A.,'Fracture prediction of a defective vessel, Preliminary analysis', E93711C, Materials Technology Centre, 1990.

2. Smith, N., 'ECA Final Report' to be published.

3. Garwood, S.J., Gordon, J.R., Willoughby, A.A., Legatt, R.H. and Jutla, T., 'Crack tip opening displacement (CTOD) methods for fracture assessments: Proposals for revisions to BSI PD 6493', Welding Inst., 1988.

4. Lamain, L.G., 'Numerical analysis in EPFM', Elastic-Plastic Fracture Mechanics, Ed. L.H. Larsson, Proc. 4th Advanced Seminar on Fracture Mechanics, Ispra, Italy, 24-28 Oct. 1983, 227-261; 1983.

5. Lemaitre, J., 'A continuous damage mechanics model for ductile fracture', J. Eng. Mat. & Tech., Trans ASME, 107:83-89; 1985.

6. Faupel, J.H., 'Yield and bursting characteristics of heavy-wall cylinders', Trans ASME, 78:5:1031-1064; 1956.

7. Karami, G. and Fenner, R.T., 'Analysis of mixed mode fracture and crack closure using the boundary integral equation method', Int. J. Fract., 30:13-29; 1986.

8. Mudry, F., 'Methodology and applications of local criteria for the prediction of ductile tearing' Elastic-Plastic Fracture Mechanics, Ed.L.H. Larsson, Proc. 4th Advanced Seminar on Fracture Mechanics, Ispra, Italy, 24-28 Oct. 1983, 263-283; 1983.

9. Shih, C.F. and German, M.D., 'Requirements for a one parameter characterization of crack tip fields by the HRR Singularity', Int . J. Fract., 17:1:27-43; 1981.

10. McDill, M., Goldak, J., Oddy, A. and Bibby, M., 'Isoparametric quadrilaterals and hexahedrons for mesh-grading algorithms', Comm. Appl. Num. Meth., 3:155-163; 1987.

11. McDill, M., Goldak, J. and Oddy, A., 'An adaptive mesh-management algorithm for three-dimensional automatic finite element analysis', 12th Canadian Congress of Applied Mechanics, Ottawa, 766-767; 1989.

12. Saarenheimo, A., Talja, H., Ikonen, K., Rintamaa, R., Keinanen, H. and Torronen, K., 'Fracture behaviour simulation of a flawed full scale pressure vessel', Int. J. Press. Ves. & Piping, 41:1:75-101; 1990.

13. Truitt, J.B. and Raju, P.P., 'Three-dimensional versus axisymmetric finite-element analysis of a cylindrical vessel inlet nozzle subject to internal pressure - A comparative study', J. Press. Ves. Tech., Trans ASME, 100:134-140; 1978.

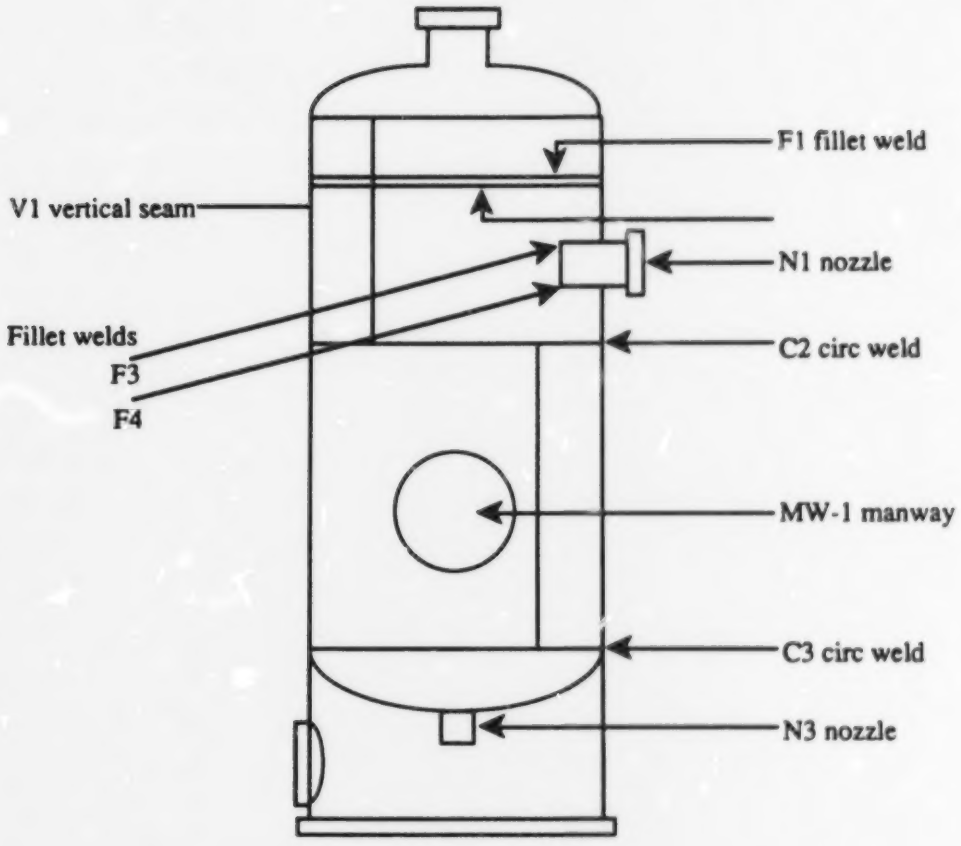

Weld identification	Weld type	Number of cracks	Measured length min-max (in.)
F1	Fillet	13	00.750-69.000
F2	Fillet	12	01.000-59.000
V1	Vertical seam	3	00.125-00.375
F3/F4	Attachment (fillet)	4	Not recorded
C3	Circumferential seam	5	00.250-01.000
N3	Nozzle	6	00.250-00.500
MW1	Manway nozzle	12	00.250-02.000

Notes: V1: These cracks are reported as being in the intersection of the vertical seam and the circumferential seam C2
C3: Two of the five cracks are reported as being transverse.

Fig. 1. Schematic diagram of the vessel tested. (neg 20539)

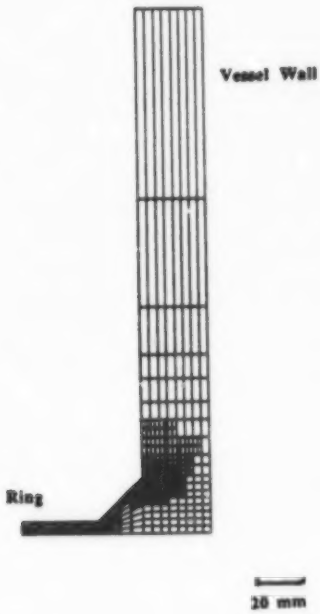

Fig. 2. Demister ring mesh. (neg 20538)

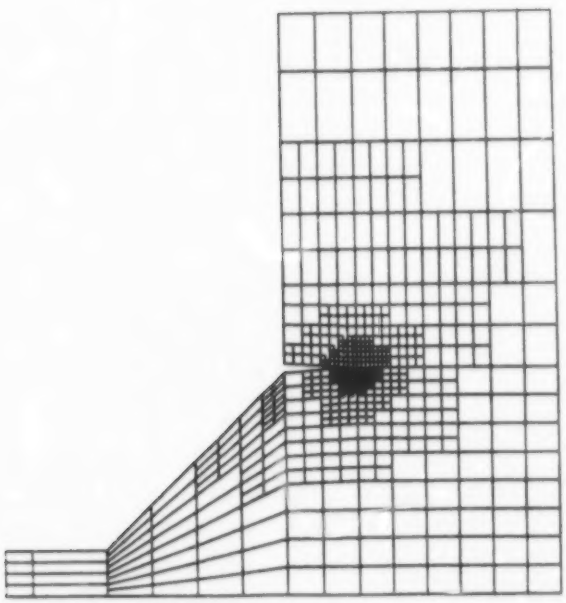

Fig. 3. Close-up view of mesh around demister ring flaw. (neg 20537)

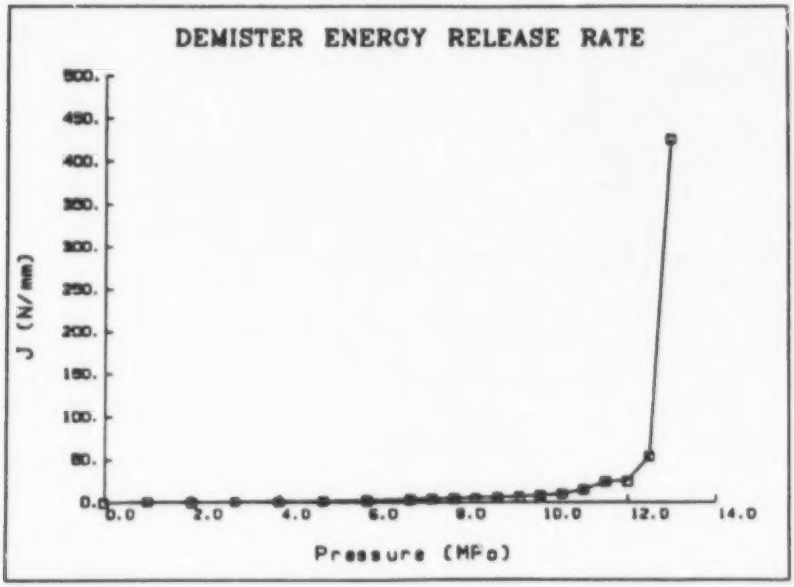

Fig. 4. Energy release rate vs applied pressure for the demister ring flaws. (neg 20536)

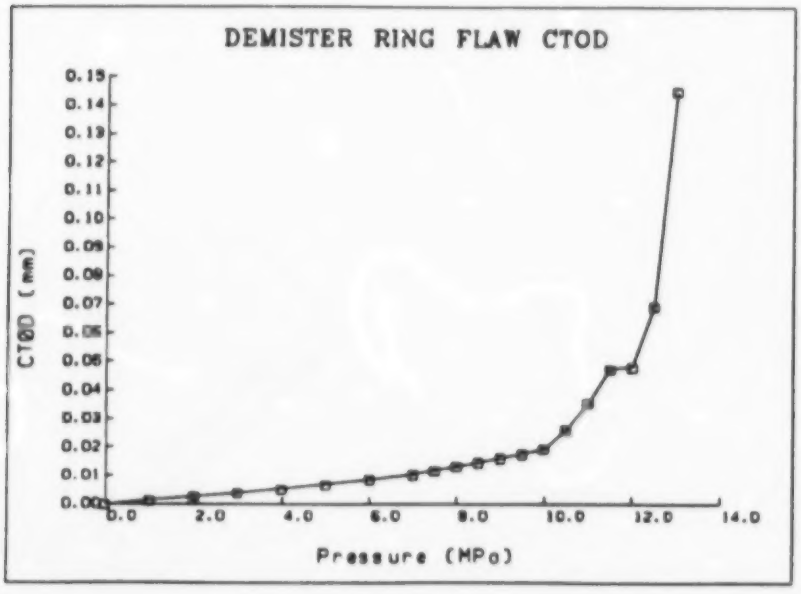

Fig. 5. Crack tip opening displacement vs pressure for the demister ring flaw. (neg 20535)

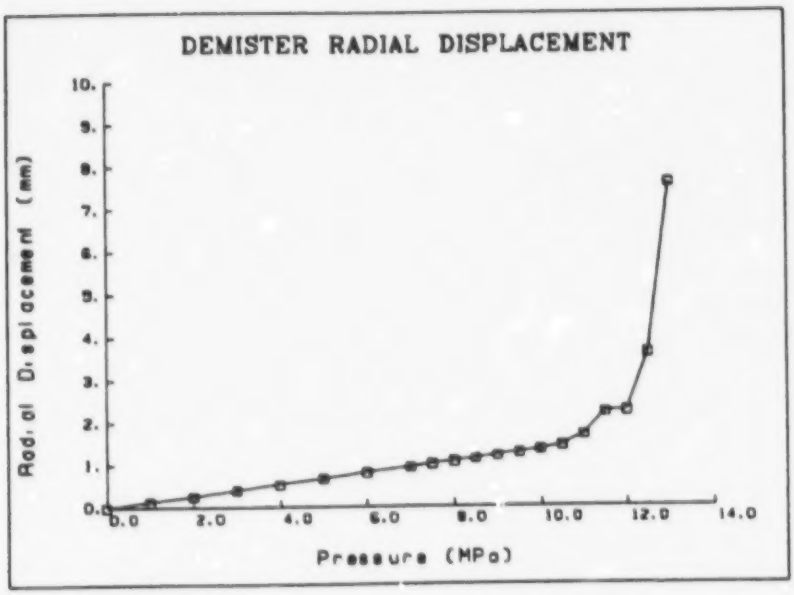

Fig. 6. Radial displacement of vessel wall vs pressure for the demister ring flaw. (neg 20534)

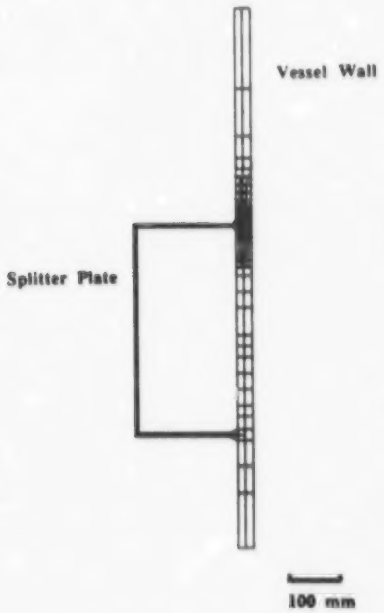

Fig. 7. Splitter plate mesh. (neg 20533)

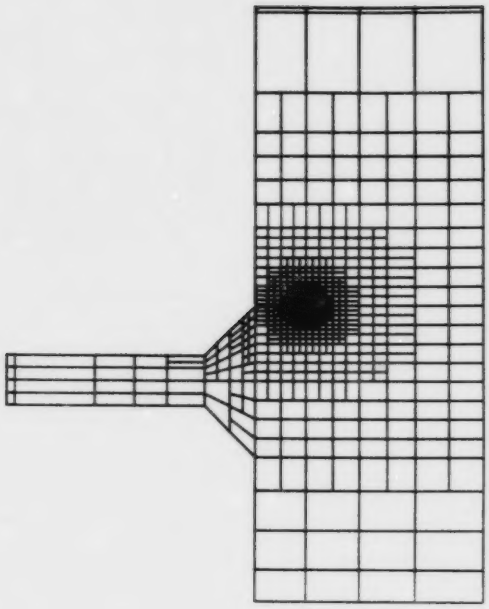

Fig. 8. Close-up view of mesh around the splitter plate flaw. (neg 20532)

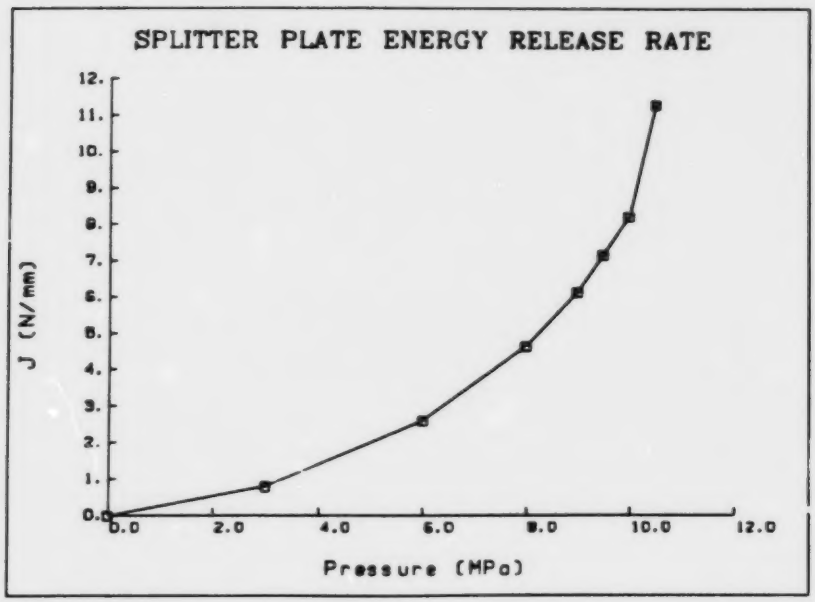

Fig. 9. Energy release rate vs applied pressure for the splitter plate flaws. (neg 20530)

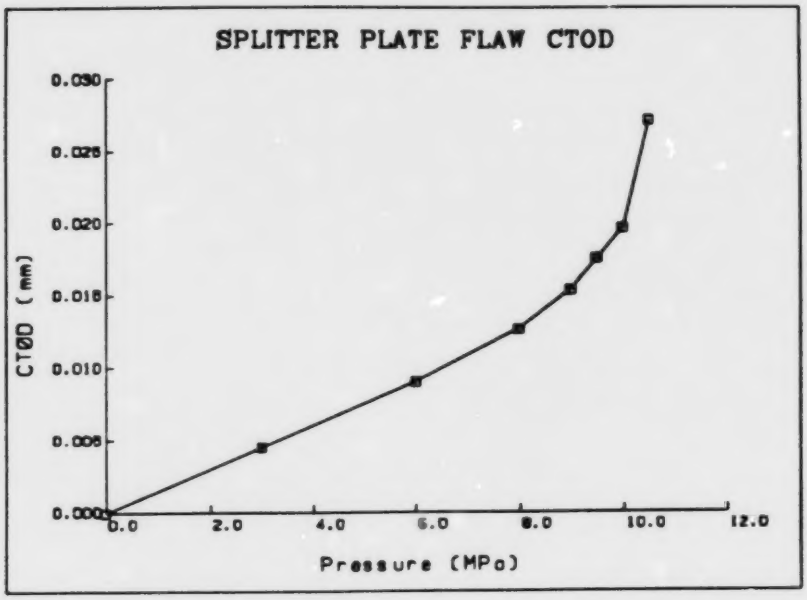

Fig. 10. Crack tip opening displacement vs pressure for the splitter plate flaw. (neg 20529)

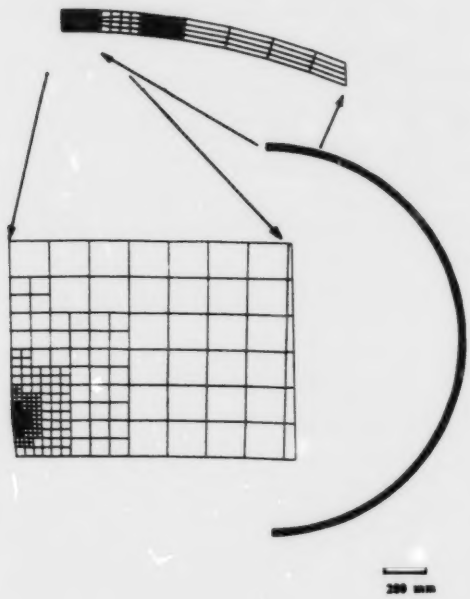

Fig. 11. Mesh used for the axial flaw in weld C1. (neg 20531)

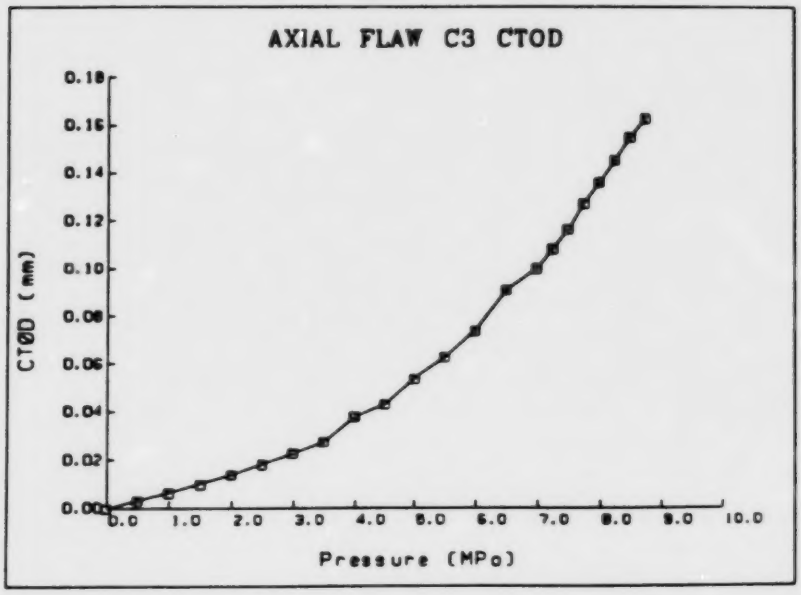

Fig. 12. Energy release rate vs applied pressure for the axial flaw in weld C1. (neg 20528)

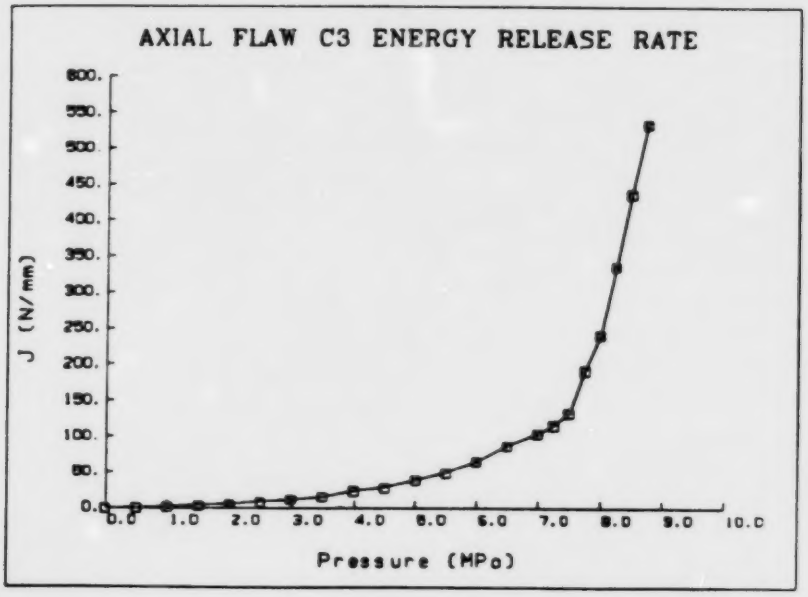

Fig. 13. Crack tip opening displacement vs pressure for the axial flaw in weld C1. (neg 20527)

Fig. 14. Magnified displacements (10x) for the axial flaw in weld C1 at 7.5 MPa. (neg 20526)

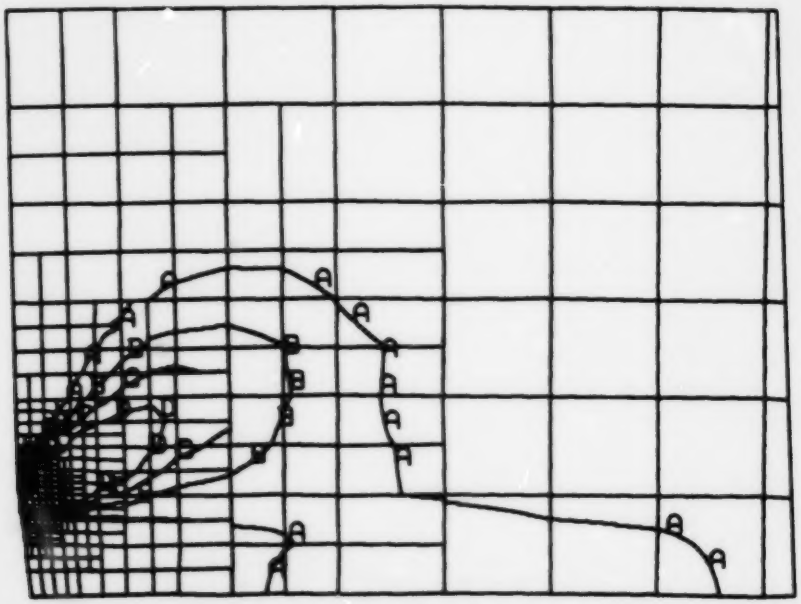

Fig. 15. Plastic zone size, axial flaw, weld C1, at 7.5 MPa. Plastic strain contour values A 0.002; B 0.004; C 0.006; D 0.008. (neg 20525)

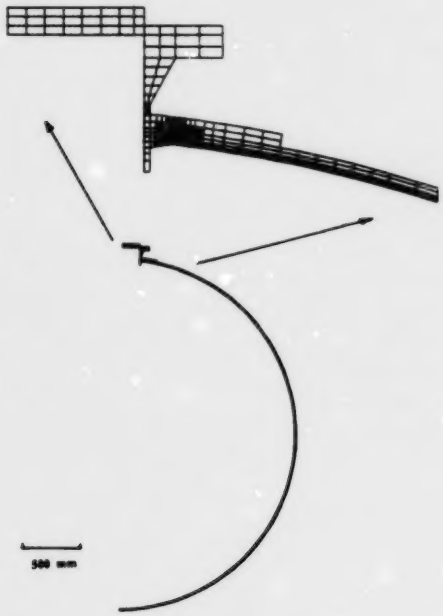

Fig. 16. Manway flaw 1 mesh, R' = 3.2R. (neg 20522)

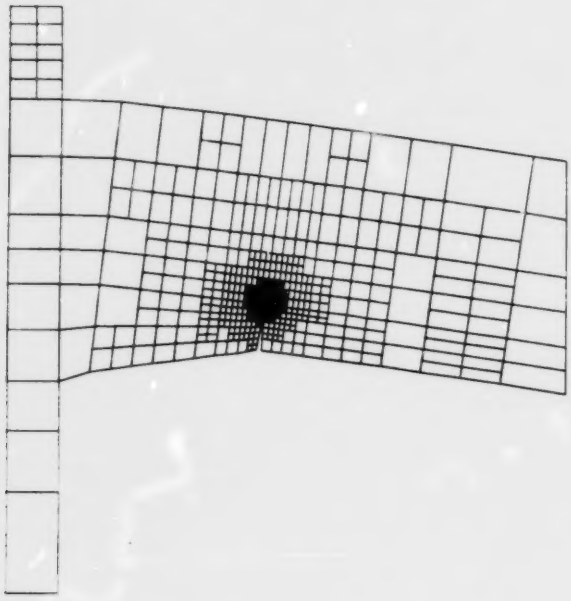

Fig. 17. Close-up view of mesh around manway flaw 1. (neg 20521)

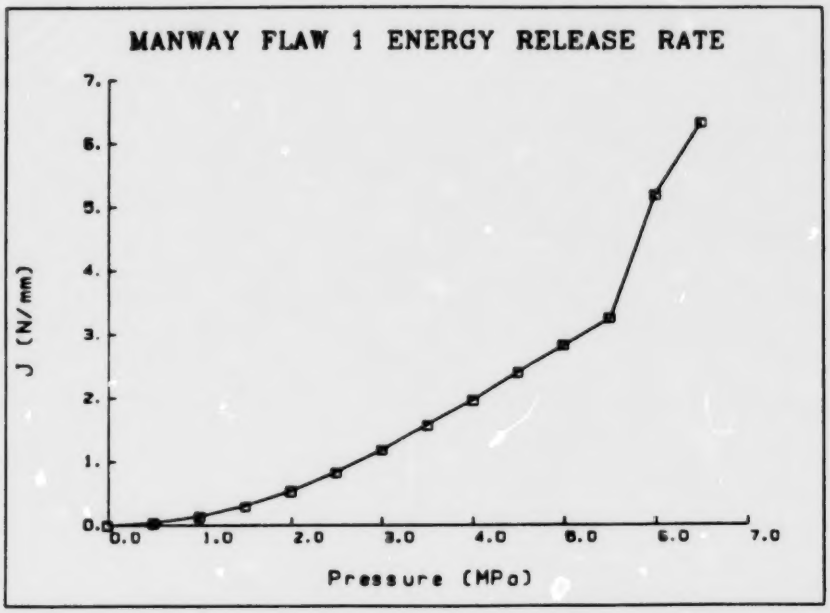

Fig. 18. Energy release rate vs applied pressure for manway flaw 1. (neg 20524)

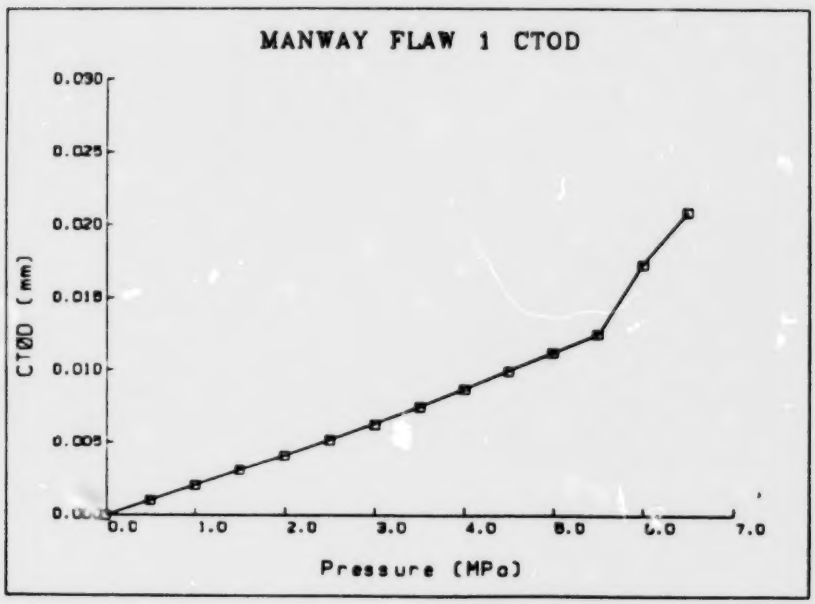

Fig. 19. Crack tip opening displacement vs pressure for manway flaw 1. (neg 20523)